Bloch oscillations of spin-orbit-coupled cold atoms in an optical lattice and spin-current generation

Wei Ji,[1] Keye Zhang,[1,3] Weiping Zhang,[2,3] and Lu Zhou[1,3,*]

[1]*State Key Laboratory of Precision Spectroscopy, Quantum Institute of Light and Atoms, School of Physics and Material Science, East China Normal University, Shanghai 200241, China*

[2]*Department of Physics and Astronomy, Shanghai Jiaotong University and Tsung-Dao Lee Institute, Shanghai 200240, China*

[3]*Collaborative Innovation Center of Extreme Optics, Shanxi University, Taiyuan, Shanxi 030006, China*

(Received 2 November 2018; published 1 February 2019)

We study the Bloch oscillation dynamics of a spin-orbit-coupled cold atomic gas trapped inside a one-dimensional optical lattice. The eigenspectra of the system is identified as two interpenetrating Wannier-Stark ladders. Based on that, we carefully analyzed the Bloch oscillation dynamics and found out that intraladder coupling between neighboring rungs of the Wannier-Stark ladder give rise to ordinary Bloch oscillation, while interladder coupling leads to small-amplitude high-frequency oscillation superimposed on it. Specifically, spin-orbit interaction breaks Galilean invariance, which can be reflected by out-of-phase oscillation of the two spin components in the accelerated frame. The possibilities of generating spin current in this system are also explored.

DOI: 10.1103/PhysRevA.99.023604

I. INTRODUCTION

Bloch oscillation describes that inside a lattice potential a particle will perform periodic oscillation instead of constant acceleration when subject to a constant external force. It was first proposed in electronic systems [1]; however it was not observed until the use of semiconductor superlattices [2] due to the small lattice constant and imperfections in conventional crystal. The frequency of Bloch oscillations is proportional to the applied force F, which can have potential applications in precision measurements. Besides that, the dynamics concerning particles moving in periodic structures is itself important because it is a pure quantum effect and reflects the properties of the energy band, such as the topology [3]. These qualities have extended people's interest in Bloch oscillation beyond electronic systems. Bloch oscillation has been experimentally observed in optical systems [4] and ultracold atoms trapped in an optical lattice [5–7]. Recently it was demonstrated that impurity moving in quantum liquids can also display the behavior of Bloch oscillation [8,9]. Theoretically, Bloch oscillation can be well understood within an adiabatical approximation in which the particles move in a Bloch energy band under the action of the force [5]. The eigenstate of Bloch oscillations is also well known as a Wannier-Stark ladder (WSL) [10].

On the other hand, besides the external center-of-mass motion, particles possess internal degrees of freedom such as the electronic spin. Pseudospin can also be constructed from the atomic internal energy-level structure. Through the mechanism of spin-orbit (SO) coupling a particle's orbital motion can be connected to its spin dynamics and lead to rich physics. Recently SO coupling has been successfully implemented in a neutral atom [11–13]. Along with that, interesting physics have been predicted in SO-coupled atomic systems, for example, dipole oscillation [11,14], *Zitterbewegung* [15,16], spin-dependent pairing [17], SO-modulated Anderson localization [18–20], SO-modulated atom optics [21], and exotic dynamics [22–26].

Then it is natural to ask how Bloch oscillation will be affected by SO interaction. In the present work we will investigate the Bloch oscillation dynamics of SO-coupled cold atoms in a one-dimensional optical lattice. An important motivation lies in the recent achievement of SO-coupled Bose-Einstein condensates (BECs) in a one-dimensional optical lattice [22], which guarantee that the results obtained here can be readily observed in experiment. In previous theoretical works, Larson and co-workers investigated Bloch oscillation of SO-coupled BEC in a two-dimensional optical lattice in which transverse spin current and atomic *Zitterbewegung* are predicted [27]. Bloch oscillation of a SO-coupled helicoidal molecule was studied by Caeteno in [28]. Kartashov *et al.* studied Bloch oscillation in one-dimensional optical and Zeeman lattices in the presence of SO coupling, where they give a detailed discussion on the amplitude and wave-packet width of Bloch oscillation [29]. Although the WSL eigenspectra were given in [29], their relation with the oscillation dynamics was not clarified. Here we solve the dynamics using the theory of WSL. We show that one can understand the properties of Bloch oscillation dynamics in the presence of SO coupling via analyzing the coupling of WSLs. Especially in the case with finite Zeeman detuning, which was not considered in [29], the two spin components will display unusual out-of-phase oscillation. In addition, we show how this can serve as an unambiguous proof of broken Galilean invariance caused by SO interaction. Since SO interaction can play a crucial role in generating and manipulating spin current [30], we will also look into the possibility of generating spin current in the present one-dimensional system.

The article is organized as follows: In Sec. II we present our model and the dynamics are solved with WSL. Section III

*Corresponding author: lzhou@phy.ecnu.edu.cn

is devoted to the detailed discussion of Bloch oscillation. The possibility of generating spin current in the present system is explored in Sec. IV. Finally, we conclude in Sec. V.

II. MODEL

As shown in Fig. 1, our model is based on the recent experiment [22] with a ^{87}Rb BEC prepared in a one-dimensional optical lattice along the z direction, inside which the effective SO interaction is induced via coupling the $|1,-1\rangle$ ($|\downarrow\rangle$) and $|1,0\rangle$ ($|\uparrow\rangle$) hyperfine states with Raman lasers. In addition to that, here we consider that a constant external force F is exerted on the atoms via tilting the optical lattice. The effective single-particle Hamiltonian reads

$$\begin{aligned}\hat{H} &= \hat{H}_{\rm SO} + U_0 \sin^2(k_l z) - Fz,\\ \hat{H}_{\rm SO} &= \frac{(p_z-\hat{A})^2}{2m} + \frac{\hbar\Omega}{2}\hat{\sigma}_x + \frac{\hbar\delta}{2}\hat{\sigma}_z,\end{aligned} \tag{1}$$

in which the SO coupling is embodied in the effective vector potential $\hat{A} = -m\alpha\hat{\sigma}_z$ ($\alpha = \hbar k_R/m$ characterizes SO coupling strength with k_R the Raman beam wave vector), Ω is the Raman coupling strength, and δ is the two-photon detuning. The periodic potential is characterized by the depth U_0 and period $d = \pi/k_l$.

By performing lowest energy-band truncation and assuming a tight-binding approximation, Hamiltonian (1) can be expanded in the σ Wannier basis $|j,\sigma\rangle$ (with j the lattice site index) as

$$\begin{aligned}\hat{H} = \sum_j \Bigg\{\Bigg[&-\frac{J}{2}\cos(\pi\gamma)\sum_\sigma |j,\sigma\rangle\langle j+1,\sigma| + i\frac{J}{2}\sin(\pi\gamma)\\ &\times(|j,\uparrow\rangle\langle j+1,\uparrow| - |j,\downarrow\rangle\langle j+1,\downarrow|) + \frac{\hbar\Omega}{2}|j,\uparrow\rangle\\ &\times\langle j,\downarrow| + \text{H.c.}\Bigg] - Fd\sum_\sigma j|j,\sigma\rangle\langle j,\sigma| + \frac{\hbar\delta}{2}(|j,\uparrow\rangle\\ &\times\langle j,\uparrow| - |j,\downarrow\rangle\langle j,\downarrow|)\Bigg\},\end{aligned} \tag{2}$$

in which the spin-dependent hopping matrix element $\hat{T} = J\exp(-i/\hbar\int\hat{A}dl)/2$ is obtained through Peierls substitution [31], J is the tunneling amplitude without SO coupling, $\gamma = k_R/k_l$. J can be calculated as

$$J = -2\int dz w_{j+1}(z)\left[-\frac{d^2}{dz^2} + U_0\sin^2(k_l z)\right]w_j(z), \tag{3}$$

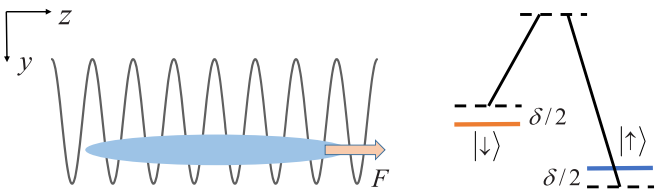

FIG. 1. Schematic diagram showing the system under consideration.

with $w_j(z) = w(z - z_j)$ the Wannier state of the lowest energy band at the jth site, which can be obtained numerically [32]. Here we consider the case of $U_0 > 0$ with $z_j = jd$.

In order to find out the eigenstates of Hamiltonian (2), it will be more convenient to transform it into the Bloch basis via the Fourier transformation [33]

$$|q,\sigma\rangle = \sqrt{\frac{d}{2\pi}}\sum_{j=-\infty}^{\infty}|j,\sigma\rangle e^{iqjd}. \tag{4}$$

One can then obtain

$$\hat{H}(q) = \langle q|\hat{H}|q\rangle = \begin{pmatrix} H_d^+ & \hbar\Omega/2\\ \hbar\Omega/2 & H_d^-\end{pmatrix}, \tag{5}$$

with $H_d^\pm = -J\cos(qd \mp \pi\gamma) \pm \hbar\delta/2 - iF\partial/\partial q$. The eigenvalue problem then becomes

$$\begin{aligned}&-iF\frac{\partial\psi_\uparrow(q)}{\partial q} - J\cos(qd-\pi\gamma)\psi_\uparrow(q)\\ &\quad+\frac{\hbar\delta}{2}\psi_\uparrow(q)+\frac{\hbar\Omega}{2}\psi_\downarrow(q) = E\psi_\uparrow(q),\end{aligned} \tag{6a}$$

$$\begin{aligned}&-iF\frac{\partial\psi_\downarrow(q)}{\partial q} - J\cos(qd+\pi\gamma)\psi_\downarrow(q)\\ &\quad-\frac{\hbar\delta}{2}\psi_\downarrow(q)+\frac{\hbar\Omega}{2}\psi_\uparrow(q) = E\psi_\downarrow(q),\end{aligned} \tag{6b}$$

where $\psi(q) = [\psi_\uparrow(q), \psi_\downarrow(q)]^T$ is the eigenvector.

Consider that $\psi^\nu(q) = [\psi_\uparrow^\nu(q), \psi_\downarrow^\nu(q)]^T$ is the νth eigensolution of Eqs. (6) with the corresponding eigenvalue E_ν, which can be solved via performing the Fourier expansion

$$\begin{aligned}\psi_\uparrow^\nu(q) &= \sqrt{\frac{d}{2\pi}}\sum_{m=-M}^{M}A_m^\nu\exp\left[iqmd + i\frac{J}{Fd}\sin(qd-\pi\gamma)\right],\\ \psi_\downarrow^\nu(q) &= \sqrt{\frac{d}{2\pi}}\sum_{m=-M}^{M}B_m^\nu\exp\left[iqmd + i\frac{J}{Fd}\sin(qd+\pi\gamma)\right],\end{aligned} \tag{7}$$

where A_m^ν and B_m^ν are expansion coefficients with the truncation number M. Through numerical calculation we found $M = 50$ to be a good approximation for the parameters considered in the present work. Substitute (7) into Eqs. (6), and one can have

$$\begin{aligned}&\frac{\hbar\Omega}{2}\sum_{m'}i^{m-m'}J_{m-m'}\left(\frac{2J}{Fd}\sin(\pi\gamma)\right)B_{m'}^\nu\\ &\quad+\left(mFd+\frac{\hbar\delta}{2}\right)A_m^\nu = E_\nu A_m^\nu,\\ &\frac{\hbar\Omega}{2}\sum_{m'}(-i)^{m-m'}J_{m-m'}\left(\frac{2J}{Fd}\sin(\pi\gamma)\right)A_{m'}^\nu\\ &\quad+\left(mFd-\frac{\hbar\delta}{2}\right)B_m^\nu = E_\nu B_m^\nu,\end{aligned} \tag{8}$$

with $J_n(z)$ the nth-order Bessel functions of the first kind. One can then numerically solve Eqs. (8) and obtain the coefficients A_m^ν, B_m^ν and the corresponding eigenenergy E_ν. The Wannier

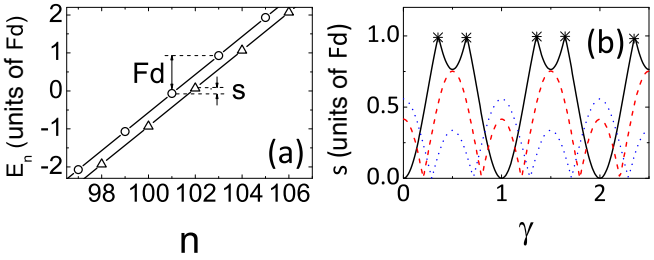

FIG. 2. (a) Eigenenergy spectra of the system under consideration. The spectra consists of two interpenetrating WSL; the intraladder spacing of both ladders is Fd while the interladder spacing is s. (b) s vs γ at $\delta = 0$ (black solid line), $\delta = 0.2\Omega$ (red dashed line) and $\delta = 0.5\Omega$ (blue dotted line). The asterisks mark the values of γ at which $s = Fd$. The other parameters are set as $J = 10Fd$ and $\hbar\Omega = 80Fd$.

amplitudes of the corresponding eigenvector read

$$W^{\nu}_{j,\uparrow} = \sum_m A^{\nu}_m J_{-j-m}\left(\frac{J}{Fd}\right)e^{i(j+m)\pi\gamma},$$
$$W^{\nu}_{j,\downarrow} = \sum_m B^{\nu}_m J_{-j-m}\left(\frac{J}{Fd}\right)e^{-i(j+m)\pi\gamma}. \quad (9)$$

In the case without SO coupling the eigenenergy of Eqs. (6) is known as WSL [34], which consists of quantized energy levels with equal energy spacing Fd. In the presence of SO coupling WSL still exists, as can be seen from the Hamiltonian (1) with $\hat{H}(z)\psi(z+d) = (E+Fd)\psi(z+d)$. However, the coupling between two pseudospin states will lead to two interpenetrating WSL positioned symmetrically around 0 [29] with an intraladder separation s, as shown in Fig. 2(a). The interladder spacing within the two WSL is still Fd. By considering that, we can label the WSL eigenenergy with $\nu_{1(2)}$ and $E_{\nu_{1(2)}} = \nu_{1(2)}Fd \mp s/2$. The intraladder spacing s is a composite function of γ, Ω, and δ. As shown in Fig. 2(b), s is a periodic function of γ. When $\delta = 0$, $s = 0$ for integer values of γ, the two WSL overlaps. This can be seen because Eqs. 6(a) and 6(b) are the same by replacing $\psi_\uparrow(q) \to \psi_\downarrow(q)$ at $\delta = 0$ and the integer γ, signaling identical dynamics for the two spin components. Interestingly, in addition to that, at some specific values of γ marked by asterisks in Fig. 2(b), $s = Fd$, also indicating overlapping WSL. A nonzero δ separates the two ladders even at $\gamma = 0$.

The relation between the WSL spectrum and dynamics can be understood from the mean velocity. The velocity operator can be defined as $d\hat{z}/dt = i[\hat{H}, \hat{z}]/\hbar$ using the Hamiltonian (2), and assuming the atomic wave function $|\psi(t)\rangle = \sum_{j,\sigma}\psi_{j,\sigma}(t)|j,\sigma\rangle$, one can calculate the mean velocity as

$$\frac{dz}{dt} = \frac{Jd}{\hbar}\sum_j \mathrm{Im}[e^{-i\pi\gamma}\psi^*_{j,\uparrow}(t)\psi_{j+1,\uparrow}(t) + e^{i\pi\gamma}\psi^*_{j,\downarrow}(t)\psi_{j+1,\downarrow}(t)]. \quad (10)$$

Then one can take advantage of Wannier-Stark eigenstates by considering that $\psi_{j,\sigma}(t) = \sum_\nu a_\nu W^{\nu}_{j,\sigma}\exp(-iE_\nu t/\hbar)$ with $a_\nu = \sum_{j,\sigma} W^{\nu*}_{j,\sigma}\psi_{j,\sigma}(0)$, and the mean velocity can be expressed as

$$\frac{dz}{dt} = \frac{Jd}{\hbar}\sum_{\nu,\nu'}\mathrm{Im}\left\{a^*_\nu a_{\nu'}\left[\sum_j W^{\nu*}_{j,\uparrow}W^{\nu'}_{j+1,\uparrow}e^{-i\pi\gamma} + \sum_j W^{\nu*}_{j,\downarrow}W^{\nu'}_{j+1,\downarrow}e^{i\pi\gamma}\right]e^{i(E_\nu - E_{\nu'})t/\hbar}\right\}. \quad (11)$$

The particle mean position $z(t) = z_\uparrow(t) + z_\downarrow(t)$ can then be derived via integrating Eq. (11) over time, in which

$$z_{\uparrow(\downarrow)}(t) = \sum_{\nu\neq\nu'}\frac{Jd}{E_\nu - E_{\nu'}}\mathrm{Re}\left\{a^*_\nu a_{\nu'}\sum_j W^{\nu*}_{j,\uparrow(\downarrow)}W^{\nu'}_{j+1,\uparrow(\downarrow)}e^{\mp i\pi\gamma} \times [1 - e^{i(E_\nu - E_{\nu'})t/\hbar}]\right\} + z_{\uparrow(\downarrow)}(0) \quad (12)$$

indicates the mean position of spin-σ component. Equation (12) predicts that the oscillation frequencies are ruled by the energy difference between the two Wannier-Stark levels with the amplitude of each frequency inversely proportional to the energy distance of those Wannier-Stark states and proportional to the overlap of their wave functions.

In the absence of SO coupling it is well known that the Wannier-Stark eigenstate W^{ν}_j has the form of a Bessel function of the first kind ($J_{\nu+j}(z)$) with $W^{\nu}_{j+1} = W^{\nu+1}_j$ [33], and $\sum_j W^{\nu*}_j W^{\nu'}_{j+1} = \sum_j W^{\nu*}_j W^{\nu'+1}_j$ takes the value 1 for $\nu = \nu' + 1$ and 0 otherwise. This indicates that in the oscillation dynamics each rung of the WSL is coupled only to its neighboring rung with the Bloch frequency $\omega_B = (E_\nu - E_{\nu'})/\hbar = Fd/\hbar = 2\pi/T_B$. Note that in the presence of SO coupling the coupled equations (8) indicate two WSLs in which any rung of the ladder is coupled to all the rungs of the other ladder, which will substantially modify the Bloch oscillation dynamics. This will be discussed in detail in the subsequent section.

III. BLOCH OSCILLATION DYNAMICS

The Bloch oscillation dynamics have been studied in [29] for the case of $\delta = 0$. The results predicted there can be well understood under adiabatical theory. When F is weak enough not to induce interband transitions, the adiabatic approximation can be applied, under which the atoms move adiabatically along the energy band with the quasimomentum $q(t) = q(0) + Ft/\hbar$. One can predict that the frequency of Bloch oscillation is proportional to Fd, with the amplitude proportional to the bandwidth. The properties of Bloch oscillation can then be captured via further looking into the energy-band structure, which can be obtained through diagonalizing the Hamiltonian (5) without the force ($F = 0$). This results in a two-band structure with $\varepsilon_\pm(q) = -J\cos qd\cos\pi\gamma \pm \sqrt{J^2\sin^2 qd\sin^2\pi\gamma - \hbar\delta J\sin qd\sin\pi\gamma + \hbar^2\delta^2/4 + \hbar^2\Omega^2/4}$. Two major results are predicted in [29]: (i) In analogy to increasing the potential depth U_0 of the optical lattice, SO interaction can take the same effect of band flattening [23]. In this case the Bloch oscillation amplitude will be suppressed and thus make it difficult to measure. An example for this is

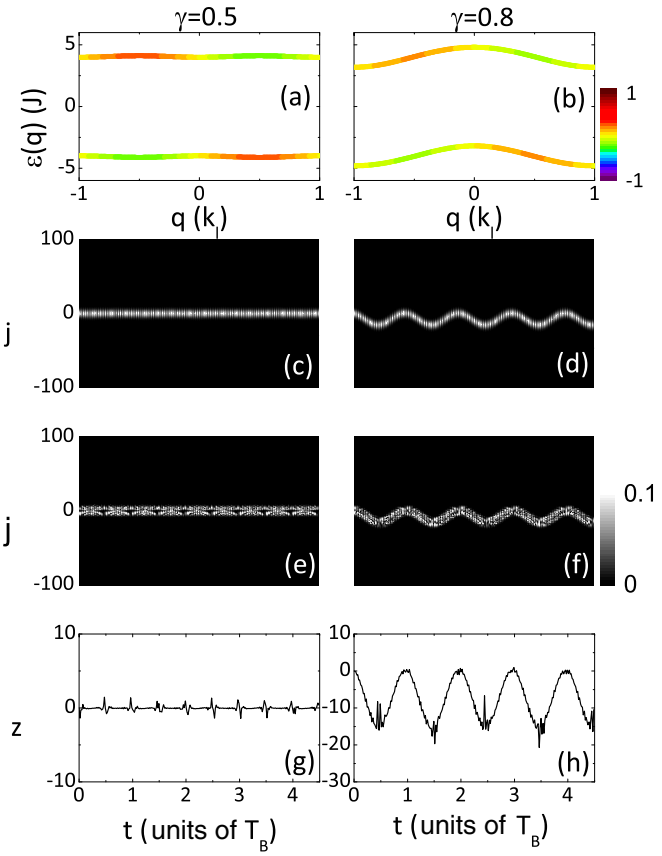

FIG. 3. (a, b) Energy band for an atom in a periodic potential $U(z) = U_0 \sin^2 k_l z$ and subject to SO interaction, with the color indicating spin polarization $\langle\hat{\sigma}_z\rangle$. (c, d) Dynamics of $|\psi_\uparrow|^2$. (e, f) Dynamics of $|\psi_\downarrow|^2$. (g, h) Dynamics of the mean position z. The left column corresponds to $\gamma = 0.5$ while the right column corresponds to $\gamma = 0.8$. The other parameters are set as $J = 10Fd$, $\hbar\Omega = 80Fd$, and $\delta = 0$.

given at $\gamma = 0.5$ with the energy band shown in Fig. 3(a). (ii) Since in the adiabatic approximation the mean velocity of the atom $v(q) = d\varepsilon(q)/\hbar dq$, the change in the band structure indicates that the atomic dynamics will be subject to strong modification. As an example, for the band profile at $\gamma = 0.8$ shown in Fig. 3(b), the initial atomic moving direction will be reversed.

These phenomena can also be explained using the theory of WSL. By considering that the eigenstate of the system consists of two interpenetrating WSL, one can group their contribution to the dynamics into two terms. Similar to the case without SO coupling, if starting from Eqs. (8) and (9) one can prove that within each ladder $W^{\nu_i}_{j+1,\sigma} = W^{\nu_i+1}_{j,\sigma}$ ($i = 1, 2$ label the two ladders) still holds true, then according to Eq. (12) one can conclude that in the presence of SO interaction the Bloch oscillation dynamics in general are still dominated by intraladder coupling between neighboring rungs within each ladder, indicating the oscillation frequency T_B. At $\delta = 0$, if due to the symmetry between spin-↑ and -↓ components we have $\sum_j |W^{\nu}_{j,\uparrow}|^2 = \sum_j |W^{\nu}_{j,\downarrow}|^2 = 1/2$, then according to Eqs. (11) and (12) one can predict that $z(t) = 0$ at $\gamma = 0.5$ and $dz/dt < 0$ at $\gamma = 0.8$ for initial small t, indicating that Bloch oscillation dynamics are substantially modified by SO interaction.

We assume that initially the atomic wave function

$$\psi_j(t=0) = (a\sqrt{\pi})^{-1/2} e^{-(j-j_0)^2/2a^2 + iq_0 jd} \begin{pmatrix} 1 \\ 0 \end{pmatrix} \tag{13}$$

is a spin-polarized Gaussian wave packet with width a, where j_0 is the center of the wave packet while q_0 denotes the initial quasi momentum. In our calculations the parameters are chosen as $j_0 = 0$ and $q_0 = 0$. The dynamics are simulated using the method of eigenstate expansion, and the results are demonstrated in Figs. 3(c)–3(f), from which one can see that the results of numerical simulation are consistent with the above theoretical analysis.

Besides intraladder coupling, interladder coupling also contributes to the oscillation dynamics. We calculate the value of $\sum_j W^{\nu_1 *}_{j,\sigma} W^{\nu_2}_{j+1,\sigma}$ and found out that for relatively large $|\nu_1 - \nu_2|$ (approaching 100) it really matters. This can be traced to the symmetry within WSL. Equation (8) indicates that if (A_m, B_m) are eigensolutions with eigenvalue E_ν, then $(-B^*_{-m}, A^*_{-m})$ are eigensolutions with eigenvalue $-E_\nu$. Due to the large energy difference of interladder coupling, it will superimpose a small-amplitude high-frequency oscillation on the dynamics dominated by intraladder coupling.

An interesting case is that at $\gamma = 0.5$; since the intraladder couplings are canceled out, then the dynamics deviating from $z = 0$ is the result of interladder coupling, which is shown in Fig. 3(g). One can observe small-amplitude high-frequency oscillations, which become prominent at around $t = nT_B/2$. Similar behavior can also be observed for $\gamma = 0.8$ in Fig. 3(h), in which the small oscillations are superimposed on the traditional Bloch oscillation.

The Klein four-group [29] or $\mathcal{CPT}$ symmetry [35] is conserved by the Hamiltonian $\hat{H}_{\rm SO} + U_0 \sin^2(k_l z)$ at $\delta = 0$, and then in the corresponding energy band the eigenfunctions are symmetric for spin ↑ and spin ↓ $[\psi_\uparrow(q) = \psi_\downarrow(-q)]$ at the center and edge of the Brillouin zone, which can also be seen from Eqs. (6). Then within adiabatical theory one can predict that $\langle\hat{\sigma}_z\rangle = 0$ when the atoms pass through the center and edge of the Brillouin zone. However, this symmetry is broken at finite δ. At finite δ the upper energy band and the lower one are shifted to opposite directions with respect to $q = 0$, as shown in Fig. 4(a). Physically this band asymmetry can be captured through Bloch oscillation via exerting force in opposite directions. The numerical results are shown in Figs. 4(b) and 4(c), in which a force F is considered to be exerted along the $+z$ and $-z$ direction, respectively. At $\delta = 0$ one would expect that these two dynamics are identical; here the different dynamics signal the energy-band asymmetry. Since the atomic initial state can be viewed as the superposition of the upper and lower eigenstate of the two bands, then in the adiabatic limit they will subject to different dispersions under the action of the force. This cannot take place at $\delta = 0$ where the energy bands are always symmetric and the two bands possess almost identical dispersion. The combined effect will lead to different oscillation dynamics for the two spin components; as we illustrated in Fig. 4(e), the dynamics become out of phase for the two spin components. One can also notice that in Fig. 4(d) the high-frequency oscillations for the two components are

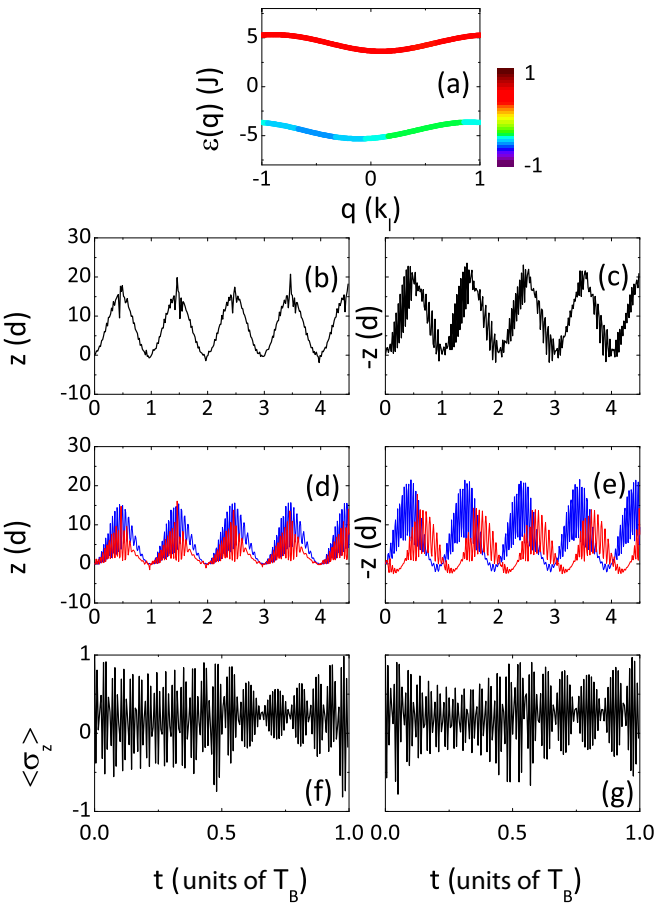

FIG. 4. (a) Asymmetric energy band at $\delta = 0.5\Omega$ with the color indicating spin polarization $\langle\hat{\sigma}_z\rangle$. (b) Dynamics of mean position z with the exerting force F along the $+z$ direction. Same dynamics of $z_\uparrow$ (blue line) and $z_\downarrow$ (red line) are shown in (d). (c, e) Same as (b) and (d) except that the force F is exerted along the $-z$ direction. (f, g) Mean value of pseudospin $\langle\hat{\sigma}_z\rangle$ vs time for the force F exerted along $+z$ and $-z$ direction, respectively. The other parameters are set as $\gamma = 0.2, J = 10Fd$, and $\hbar\Omega = 80Fd$.

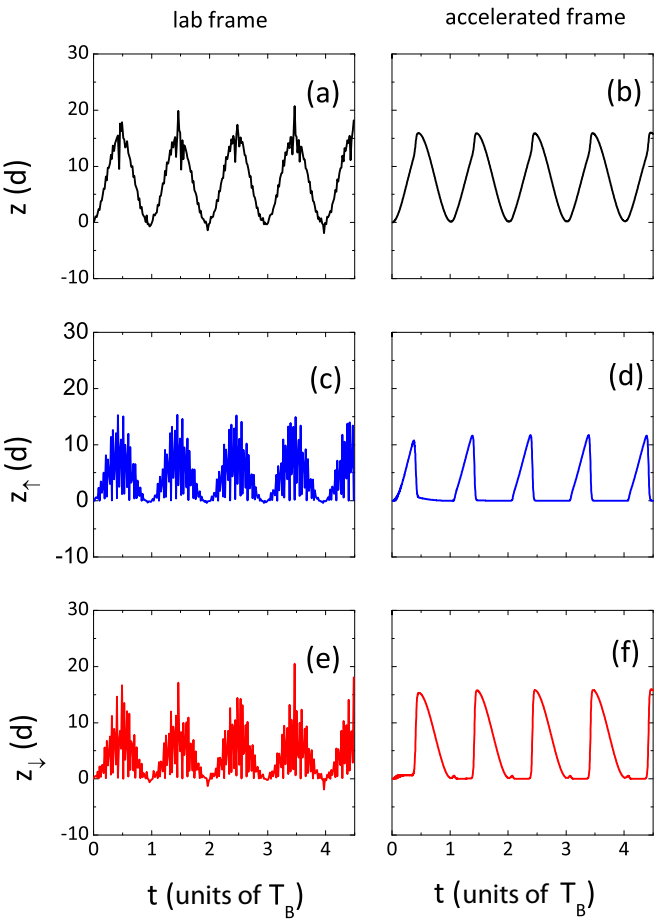

FIG. 5. Oscillation dynamics in the laboratory frame (left column) and the accelerated frame (right column). The dynamics of $z = z_\uparrow + z_\downarrow$ (first row), $z_\uparrow$ (middle row), and $z_\downarrow$ (bottom row) are shown in black, red, and blue lines, respectively. The parameters are set as $\gamma = 0.2, J = 10Fd, \delta = 0, \hbar\Omega = 80Fd$, and $E_r/J = 8.55$.

out of phase; this is because $W^{\nu*}_{j,\uparrow} W^{\nu'}_{j+1,\uparrow} = -W^{\nu*}_{j,\downarrow} W^{\nu'}_{j+1,\downarrow}$ for interladder couplings. In the meanwhile, $\langle\hat{\sigma}_z\rangle$ deviates from 0 when the wave packet passes through the center and edge of the Brillouin zone, as shown in Figs. 4(f) and 4(g).

In the case without SO coupling, one can introduce a linearly time-dependent frequency difference $\Delta\nu(t) = -Ft/md$ between the two lattice beams [5], the lattice potential becomes $U_0 \sin^2[k_l z - \pi \int_0^t d\tau \Delta\nu(\tau)]$, and in an *accelerated* frame it is equivalent to exerting a constant inertial force F on the atoms trapped in a stationary lattice. However, this equivalence cannot be established in the presence of SO coupling. This is because the SO Hamiltonian $\hat{H}_{\rm SO}$ breaks Galilean invariance as the physical momentum $p_z - \hat{A}$ does not commute with $\hat{H}_{\rm SO}$. In this case, going into a moving inertial frame will result in an additional time-dependent term $-\alpha Ft\hat{\sigma}_z$ in Hamiltonian (1), which plays the role of a time-dependent effective detuning.

We calculate the oscillation dynamics in the stationary frame (lab frame) with the exerting force F and that in the accelerated frame within which the atoms are subject to an effective force F as well as an effective time-dependent detuning $-\alpha Ft\hat{\sigma}_z$; the results are shown in Fig. 5. The dynamics in the laboratory frame are simulated with eigenstate expansion while those in the accelerated frame are calculated by means of the fourth-order Runge-Kutta method. Both initial states are given by Eq. (13). In the numerical simulation we consider the recoil energy $E_r = \hbar^2 k_l^2/2m = 8.55J$ for a typical experimental value of $U_0 = 4E_r$. As one can expect, in the laboratory frame the oscillation dynamics for spin-↑ and -↓ components are in phase, as shown in Figs. 5(c) and 5(e). However, the dynamics shown in Figs. 5(d) and 5(f) indicate that they are out of phase (phase separated in the time domain) in the accelerated frame. This interesting dynamics can be readily captured in experiment and serve as a clear proof of broken Galilean invariance, which is also the mechanism underlying other unusual behaviors such as the deviation of dipole oscillation frequency in a harmonically trapped system [11,14], the ambiguity in defining Landau critical velocity in SO-coupled condensates [36], a finite-momentum dimer bound state in a SO-coupled Fermi gas [17], and asymmetric expansion of SO-coupled atomic Bose gas [25]. The effect of broken Galilean invariance can be signified via introducing a

frequency difference between the two laser beams forming the optical lattice [22].

IV. SPIN-CURRENT GENERATION

An interesting question is how to create a spin current with SO coupling [30]. Spin currents have been experimentally generated in a SO-coupled BEC via spin Hall effect [37] and quenching [38]. In theory, Larson *et al.* studied Bloch oscillations of atomic BEC in a tilted two-dimensional (2D) optical lattice [27], in which the atoms are subject to a 2D SO interaction $\hat{H}_{\rm SO} \propto \hat{p}_x\hat{\sigma}_x + \hat{p}_y\hat{\sigma}_y$ and in turn give rise to a spin-dependent effective force proportional to $\hat{\sigma}_z$. As a result, an oscillating transverse spin current can be generated. For the present one-dimensional (1D) system we have

$$\hat{F}_z = [\hat{H}_{\rm SO}, [\hat{\mathbf{z}}, \hat{H}_{\rm SO}]] = \frac{\hbar^3 k_R \Omega}{m}\hat{\sigma}_y \mathbf{e}_z, \tag{14}$$

indicating an SO-aroused effective force along $\mathbf{e}_z$ direction and proportional to $\hat{\sigma}_y$.

Here we would like to explore the possibility of generating spin current in the present 1D system with this effective force. As suggested by Shi *et al.* [39], the spin-current operator along the z direction can be defined as

$$\hat{\jmath}_S^i(t) = \frac{d}{dt}(\hat{\sigma}_i\hat{z}). \tag{15}$$

Following a very similar procedure as when deducing Eqs. (10) and (11), and making use of the WSL eigenstate, the mean value of the σ_z component of the spin current can be calculated as

$$\begin{aligned} J_S^z(t) = \sum_j {\rm Im}\Big[& \frac{Jd}{\hbar} e^{-i\pi\gamma}\psi_{j,\uparrow}^*(t)\psi_{j+1,\uparrow}(t) \\ & - \frac{Jd}{\hbar} e^{i\pi\gamma}\psi_{j,\downarrow}^*(t)\psi_{j+1,\downarrow}(t) + 2\Omega d j \psi_{j,\uparrow}^*(t)\psi_{j,\downarrow}(t)\Big] \\ = \sum_{\nu,\nu'} {\rm Im}\Big\{ & a_\nu^* a_{\nu'} \sum_j \Big[\frac{Jd}{\hbar} W_{j,\uparrow}^{\nu *} W_{j+1,\uparrow}^{\nu'} e^{-i\pi\gamma} \\ & - \frac{Jd}{\hbar} W_{j,\downarrow}^{\nu *} W_{j+1,\downarrow}^{\nu'} e^{i\pi\gamma} + 2\Omega d j W_{j,\uparrow}^{\nu *} W_{j,\downarrow}^{\nu'}\Big] e^{i(E_\nu - E_{\nu'})t/\hbar}\Big\}, \end{aligned} \tag{16}$$

which predicts that in addition to the coupling between different rungs, the last term in Eq. (16) indicates that the coupling between spin-↑ and -↓ components also contributes to the spin current, resulting from the effective force $\hat{F}_z$ being proportional to $\hat{\sigma}_y$.

In order to illustrate the contribution of this term, one can choose $\gamma = 1$, at which the major intraladder contribution from the first two terms in Eq. (16) are canceled out at $\delta = 0$ due to the symmetry. Physically, it is equivalent to the two spin components performing identical Bloch oscillation and in the meanwhile is subject to on-site Raman coupling, as one can see from the Hamiltonian (2). In the case $\langle\hat{\sigma}_z\rangle = 0$ for the Bloch eigenstate without the force, we then numerically calculate $J_S^z(t)$ and the results are shown in Fig. 6. One can expect that in the absence of Raman coupling no spin current

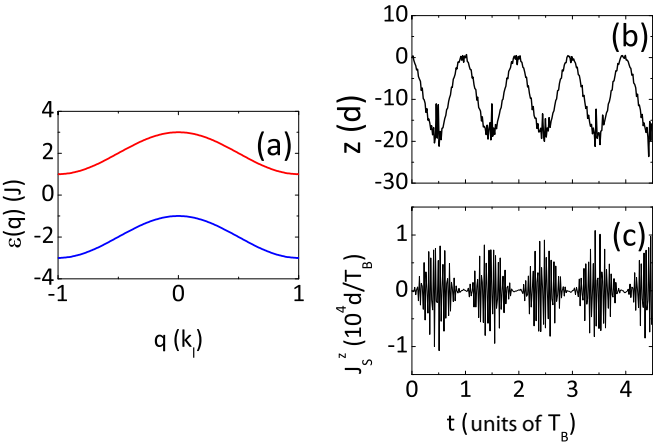

FIG. 6. (a) Energy band at $\gamma = 1$ and $\delta = 0$. (b) Dynamics of mean position z. (c) Dynamics of the spin current J_S^z. The parameters are set as $J = 10Fd$ and $\hbar\Omega = 80Fd$, with the atoms initially prepared in a Gaussian wave packet (13).

can be generated since the spin-↑ and spin-↓ components both move adiabatically along the energy band and exhibit typical properties of Bloch oscillation, as can be seen from Figs. 6(a) and 6(b). The small-amplitude high-frequency oscillation is aroused by interladder coupling, as we discussed in Sec. III. The time evolution of spin current J_S^z exhibits the behavior of collapse and revival shown in Fig. 6(c), reminiscent of the Jaynes-Cummings model in quantum optics [40]. This collapse-and-revival behavior can be understood to be as a result of the complex interplay between the external force F and the intrinsic force $F_{\rm SO} = \hbar k_R \Omega\hat{\sigma}_y/2$ aroused by SO interaction. One can also understand this collapse-and-revival behavior the same as *Zitterbewegung* [27]. *Zitterbewegung* results from coherent coupling between eigenstates of a Dirac cone with different helicity [41] and has been successfully observed in experiment with cold atoms [15,16], while here the trembling oscillation is aroused by spin swapping.

We also examined the case with finite Zeeman detuning. As one can expect, although the spin-↑ and spin-↓ components are performing different oscillations, it will be immersed in the dynamics aroused by Raman coupling and in general the spin current will exhibit the dynamics of collapse and revival. In order to achieve a constant directional spin current, one can either adapt time-dependent SO coupling [42] or unbiased external force [43].

V. SUMMARY AND OUTLOOK

Before concluding the paper, we need to note that in the presence of SO interaction one should be very careful while using the above lowest energy-band truncation. As was pointed out by Zhou and Cui [44], in this case tight-binding models have limitations in predicting the correct single-particle physics due to the missed high-band contributions. Physically the Raman lasers inducing SO interaction also inevitably couple atoms to high-lying bands, which will significantly affect the single-particle physics [24]. Experimentally, atomic BEC can also be prepared in excited bands of an optical lattice [45]. Ao and Rammer also pointed out

that high-band contributions can substantially affect the Bloch oscillation dynamics [46]. Contributions from higher Bloch bands will be important and interesting in orbital optical lattices [47]. By considering that, we compared the results presented in this work with those obtained through numerical simulation of the corresponding Schrödinger equation and found good agreement in the case of a large energy gap and small external force.

In summary, we have studied the Bloch oscillation dynamics of a SO-coupled cold atomic gas trapped inside a 1D optical lattice. The eigenspectra of the system have been identified as two interpenetrating WSL. The Bloch oscillation dynamics in this system can be well understood via analyzing the coupling between different rungs of the WSL. In the presence of finite Zeeman detuning, we show that the two spin components can display out-of-phase oscillation. This can also serve as an unambiguous proof of broken Galilean invariance aroused by SO coupling. In addition to that, we numerically explored the possibility of generating spin current in the present system. Since SO interaction has been implemented in BEC in a 1D optical lattice [22], our findings of the interesting dynamical phenomena should be within reach of present-day experiments. For BEC it will be interesting to study the impact of interparticle collisions on Bloch oscillation [48] and spin-current generation, which can be investigated by the Gaussian variational approach [49,50]. It will also be interesting to investigate Landau-Zener tunneling [51,52]. These will be left for further investigation.

ACKNOWLEDGMENTS

We thank Han Pu and Yongping Zhang for careful reading and many helpful comments on the manuscript. This work is supported by the National Natural Science Foundation of China (Grants No. 11374003, No. 11774093, No. 11574086, No. 91436211, and No. 11654005), the National Key Research and Development Program of China (Grant No. 2016YFA0302001), the Shanghai Rising-Star Program (Grant No. 16QA1401600), and the Science and Technology Commission of Shanghai Municipality (Grants No. 16DZ2260200 and No. 16ZR1409800).

[1] F. Bloch, Z. Phys. **52**, 555 (1929); C. Zener, Proc. R. Soc. London A **145**, 523 (1934).
[2] C. Waschke, H. G. Roskos, R. Schwedler, K. Leo, H. Kurz, and K. Köhler, Phys. Rev. Lett. **70**, 3319 (1993).
[3] L.-K. Lim, J.-N. Fuchs, and G. Montambaux, Phys. Rev. Lett. **108**, 175303 (2012); Y.-Q. Wang and X.-J. Liu, Phys. Rev. A **94**, 031603(R) (2016).
[4] T. Pertsch, P. Dannberg, W. Elflein, A. Bräuer, and F. Lederer, Phys. Rev. Lett. **83**, 4752 (1999); Y. Zhang, D. Zhang, Z. Zhang, C. Li, Y. Zhang, F. Li, M. R. Belić, and M. Xiao, Optica **4**, 571 (2017).
[5] M. Ben Dahan, E. Peik, J. Reichel, Y. Castin, and C. Salomon, Phys. Rev. Lett. **76**, 4508 (1996); E. Peik, M. Ben Dahan, I. Bouchoule, Y. Castin, and C. Salomon, Phys. Rev. A **55**, 2989 (1997).
[6] Q. Niu, X.-G. Zhao, G. A. Georgakis, and M. G. Raizen, Phys. Rev. Lett. **76**, 4504 (1996); S. R. Wilkinson, C. F. Bharucha, K. W. Madison, Q. Niu, and M. G. Raizen, *ibid.* **76**, 4512 (1996).
[7] For a review, see M. G. Raizen, C. Salomon, and Q. Niu, Phys. Today **50**, 30 (1997), and references therein.
[8] F. Meinert, M. Knap, E. Kirilov, K. Jag-Lauber, M. B. Zvonarev, E. Demler, and H.-C. Nägerl, Science **356**, 945 (2017).
[9] D. M. Gangardt and A. Kamenev, Phys. Rev. Lett. **102**, 070402 (2009).
[10] For a review, see M. Gluck, A. R. Kolovsky, and H. J. Korsch, Phys. Rep. **366**, 103 (2002), and references therein.
[11] J.-Y. Zhang, S.-C. Ji, Z. Chen, L. Zhang, Z.-D. Du, B. Yan, G.-S. Pan, B. Zhao, Y.-J. Deng, H. Zhai, S. Chen, and J.-W. Pan, Phys. Rev. Lett. **109**, 115301 (2012).
[12] Y.-J. Lin, K. Jiménez-Garcia, and I. B. Spielman, Nature (London) **471**, 83 (2011); P. Wang, Z.-Q. Yu, Z. Fu, J. Miao, L. Huang, S. Chai, H. Zhai, and J. Zhang, Phys. Rev. Lett. **109**, 095301 (2012); L. W. Cheuk, A. T. Sommer, Z. Hadzibabic, T. Yefsah, W. S. Bakr, and M. W. Zwierlein, *ibid.* **109**, 095302 (2012).
[13] For a review, see J. Dalibard, F. Gerbier, G. Juzeliunas, and P. Öhberg, Rev. Mod. Phys. **83**, 1523 (2011); N. Goldman, G. Juzeliūnas, P. Öhberg, and I. B. Spielman, Rep. Prog. Phys. **77**, 126401 (2014); H. Zhai, *ibid.* **78**, 026001 (2015).
[14] B. Ramachandhran, B. Opanchuk, X.-J. Liu, H. Pu, P. D. Drummond, and H. Hu, Phys. Rev. A **85**, 023606 (2012).
[15] L. J. LeBlanc, M. C. Beeler, K. J. Garcia, A. R. Perry, S. Sugawa, R. A. Williams, and I. B. Spielman, New J. Phys. **15**, 073011 (2013).
[16] C. Qu, C. Hamner, M. Gong, C. Zhang, and P. Engels, Phys. Rev. A **88**, 021604(R) (2013).
[17] L. Dong, L. Jiang, H. Hu, and H. Pu, Phys. Rev. A **87**, 043616 (2013).
[18] L. Zhou, H. Pu, and W. Zhang, Phys. Rev. A **87**, 023625 (2013).
[19] G. Orso, Phys. Rev. Lett. **118**, 105301 (2017).
[20] S. Mardonov, M. Modugno, and E. Y. Sherman, Phys. Rev. Lett. **115**, 180402 (2015).
[21] L. Zhou, J.-L. Qin, Z. Lan, G. Dong, and W. Zhang, Phys. Rev. A **91**, 031603(R) (2015); L. Zhou, R.-F. Zheng, and W. Zhang, *ibid.* **94**, 053630 (2016).
[22] C. Hamner, Y. Zhang, M. A. Khamehchi, M. J. Davis, and P. Engels, Phys. Rev. Lett. **114**, 070401 (2015).
[23] Y. Zhang and C. Zhang, Phys. Rev. A **87**, 023611 (2013).
[24] J.-S. Pan, W. Zhang, W. Yi, and G.-C. Guo, Phys. Rev. A **94**, 043619 (2016).
[25] M. A. Khamehchi, K. Hossain, M. E. Mossman, Y. Zhang, Th. Busch, M. M. Forbes, and P. Engels, Phys. Rev. Lett. **118**, 155301 (2017).
[26] Z. Lan and P. Öhberg, Phys. Rev. A **89**, 023630 (2014).
[27] J. Larson, J.-P. Martikainen, A. Collin, and E. Sjöqvist, Phys. Rev. A **82**, 043620 (2010).
[28] R. A. Caetano, Phys. Rev. B **89**, 195414 (2014).

[29] Y. V. Kartashov, V. V. Konotop, D. A. Zezyulin, and L. Torner, Phys. Rev. Lett. **117**, 215301 (2016).
[30] P. Sharma, Science **307**, 531 (2005).
[31] R. E. Peierls, Z. Phys. **80**, 763 (1933); D. R. Hofstadter, Phys. Rev. B **14**, 2239 (1976).
[32] A. A. Mostofi, J. R. Yates, Y.-S. Lee, I. Souza, D. Vanderbilt, and N. Marzari, Comput. Phys. Commun. **178**, 685 (2008); R. Walters, G. Cotugno, T. H. Johnson, S. R. Clark, and D. Jaksch, Phys. Rev. A **87**, 043613 (2013).
[33] T. Hartmann, F. Keck, H. J. Korsch, and S. Mossmann, New J. Phys. **6**, 2 (2004).
[34] G. H. Wannier, Phys. Rev. **117**, 432 (1960).
[35] V. E. Lobanov, Y. V. Kartashov, and V. V. Konotop, Phys. Rev. Lett. **112**, 180403 (2014); Y. V. Kartashov, V. V. Konotop, and D. A. Zezyulin, Europhys. Lett. **107**, 50002 (2014).
[36] Q. Zhu, C. Zhang, and B. Wu, Europhys. Lett. **100**, 50003 (2012).
[37] M. C. Beeler, R. A. Williams, K. Jiménez-García, L. J. LeBlanc, A. R. Perry, and I. B. Spielman, Nature (London) **498**, 201 (2013).
[38] C.-H. Li, C. Qu, R. J. Niffenegger, S.-J. Wang, M. He, D. B. Blasing, A. Olson, C. H. Greene, Y. Lyanda-Geller, Q. Zhou, C. Zhang, and Y. P. Chen, arXiv:1810.06504.
[39] J. Shi, P. Zhang, D. Xiao, and Q. Niu, Phys. Rev. Lett. **96**, 076604 (2006).
[40] G. Rempe, H. Walther, and N. Klein, Phys. Rev. Lett. **58**, 353 (1987).
[41] E. Schrödinger, Sitzungsber. Preuss. Akad. Wiss. Phys. Math. Kl. **24**, 418 (1930).
[42] C.-C. Chien and M. Di'Ventra, Phys. Rev. A **87**, 023609 (2013).
[43] S. Smirnov, D. Bercioux, M. Grifoni, and K. Richter, Phys. Rev. B **78**, 245323 (2008).
[44] L. Zhou and X. Cui, Phys. Rev. B **92**, 140502(R) (2015).
[45] Y. Zhai, X. Yue, Y. Wu, X. Chen, P. Zhang, and X. Zhou, Phys. Rev. A **87**, 063638 (2013).
[46] P. Ao, Phys. Rev. B **41**, 3998 (1990); P. Ao and J. Rammer, *ibid.* **44**, 11494 (1991).
[47] For a review, see T. Kock, C. Hippler, A. Ewerbeck, and A. Hemmerich, J. Phys. B **49**, 042001 (2016), and references therein.
[48] C. Gaul, E. Díaz, R. P. A. Lima, F. Domínguez-Adame, and C. A. Müller, Phys. Rev. A **84**, 053627 (2011).
[49] A. Trombettoni and A. Smerzi, Phys. Rev. Lett. **86**, 2353 (2001).
[50] Y. Cheng, G. Tang, and S. K. Adhikari, Phys. Rev. A **89**, 063602 (2014).
[51] B. Wu and Q. Niu, New J. Phys. **5**, 104 (2003).
[52] Y. Ke, X. Qin, H. Zhong, J. Huang, C. He, and C. Lee, Phys. Rev. A **91**, 053409 (2015).